ORGANOMETALLICS

Article

pubs.acs.org/Organometallics

Structures and Bonding of η^2-Bridging CO Ligands and Their Influence on the Structures and Rearrangements of Higher Nuclearity Metal Carbonyl Cluster Complexes

Richard D. Adams* and Qiang Zhang

Department of Chemistry and Biochemistry, University of South Carolina, Columbia, South Carolina 29208, United States

Supporting Information

ABSTRACT: Three products were obtained from the reaction of $IrRu_3(CO)_{13}(\mu_3\text{-H})$ with $P(Bu^t)_3$ in a hexane solution at reflux for 30 min. These have been identified as $IrRu_3(CO)_{12}[P(Bu^t)_3](\mu\text{-H})$ (**1**; 15% yield), $IrRu_2(CO)_9[P(Bu^t)_3](\mu\text{-H})$ (**2**; 29% yield), and $IrRu_3(CO)_{10}(\mu_3\text{-}\eta^2\text{-CO})[P(Bu^t)_3]_2(\mu\text{-H})$ (**3**; 19% yield). Compound **1** is simply a $P(Bu^t)_3$ derivative of $IrRu_3(CO)_{13}(\mu_3\text{-H})$. Compound **2** is electronically unsaturated and has a vacant coordination site located on the iridium atom. Compound **3** contains a butterfly tetrahedral cluster of four metal atoms with a rare η^2 triply bridging CO ligand. Compound **3** reacts with $Ru(CO)_5$ to yield the higher nuclearity cluster complex $IrRu_4(CO)_{12}(\mu_4\text{-}\eta^2\text{-CO})[P(Bu^t)_3]_2(\mu_3\text{-H})$ (**4**), which contains five metal atoms arranged in the form of an iridium-capped butterfly tetrahedron of four ruthenium atoms. Compound **4** contains a η^2-quadruply bridging CO ligand. Compound **4** reacts with CO to yield the compound $IrRu_4(CO)_{14}P(Bu^t)_3(\mu_4\text{-}\eta^2\text{-CO})(\mu\text{-H})$, **5** which contains five metal atoms in the form of a spiked-tetrahedron. Compound **5** also contains a η^2 quadruply bridging CO ligand. Compound **5** was converted to **2** in 36% yield by removal of two of the Ru groups by treatment with CO at 70 °C/10 atm. All of the new products were characterized structurally by single-crystal X-ray diffraction analyses. The η^2-coordinated bridging CO ligands serve as four-electron donors. The nature of the bonding of the different types of η^2-bridging CO ligands to the metal atoms in these clusters was investigated by DFT computational methods.

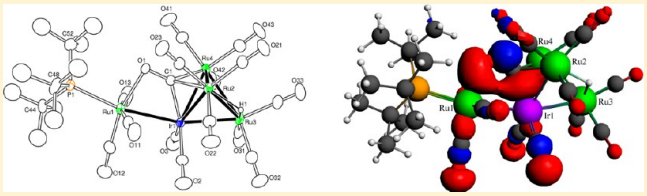

INTRODUCTION

The η^2-bridging carbonyl ligand has been shown to exist in a number of different coordination modes in polynuclear metal carbonyl complexes. In general, it serves as a four-electron donor, as represented by the structures **A**,[1] **C**,[2] **E**,[3] and **F**,[4] but on rare occasions, it can even serve as a six-electron donor, as found in the structures **B**[5] and **G**[6] (see Scheme 1). There is evidence that quadruply bridging CO ligands, such as **E**, are precursors to carbido ligands via cleavage of the CO bond,[6] and the ability of the CO ligand to adopt various bridging coordinations could play a role in the growth and transformations of polynuclear metal complexes, particularly when the transformations are accompanied by the addition or elimination of other CO ligands.[7] Multicenter coordination to metal atoms has been shown to modify the reactivity of the CO ligand.[6d] This is also central to the transformations of CO on surfaces[8] and in heterogeneous catalysis.[9]

Scheme 1. Bonding Modes of the η^2-Bridging Carbonyl Ligand in Various Metal Cluster Complexes

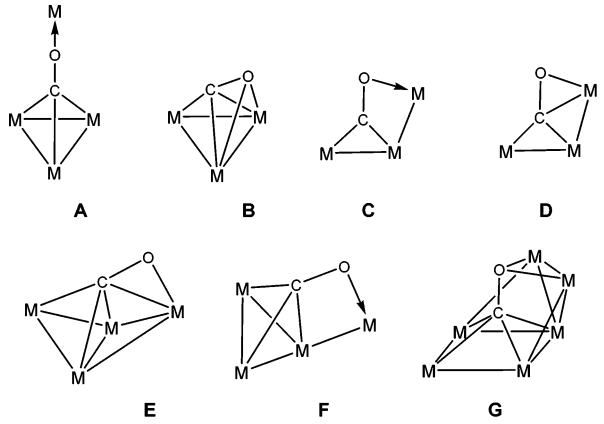

Studies have shown that certain bimetallic cluster complexes exhibit catalytic activity that is superior to that of their homonuclear components.[10,11] The $IrRu_3$ complex $IrRu_3(CO)_{13}(\mu_3\text{-H})$[12] is a precursor to an effective homogeneous bimetallic catalyst for the selective hydrogenation of alkynes.[11] We have recently shown that $IrRu_3(CO)_{13}(\mu_3\text{-H})$ reacts with $HGePh_3$ in a cluster-opening process to yield the complex $IrRu_3(CO)_{11}(GePh_3)_3(\mu\text{-H})_4$, which subsequently cleaves five phenyl groups from the three $GePh_3$ ligands to yield the bis-germylyne complex $IrRu_3(CO)_9(\mu\text{-}\eta^2\text{-}C_6H_5)(\mu_4\text{-GePh})_2(\mu\text{-}GePh_2)$ when it is heated (Scheme 2).[13]

We have now investigated the reaction of $IrRu_3(CO)_{13}(\mu_3\text{-H})$ with the sterically encumbered phosphine $P(Bu^t)_3$. Three

Received: July 23, 2013
Published: September 9, 2013

Scheme 2. Formation of a μ-η^2-Phenyl Ligand in an Ir−Ru Cluster Complex

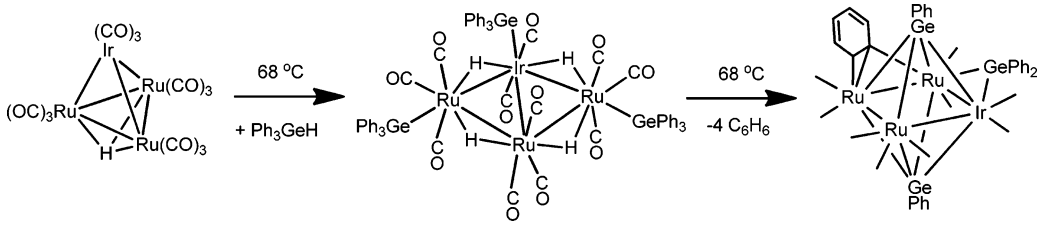

new compounds, including the unsaturated $IrRu_2$ complex $IrRu_2(CO)_9[P(Bu^t)_3](\mu\text{-}H)$ (**2**) and $IrRu_3(CO)_{10}(\mu_3\text{-}\eta^2\text{-}CO)[P(Bu^t)_3]_2(\mu\text{-}H)$ (**3**), which contains one of the rare μ_3-η^2-CO ligands **D**, have been obtained. Compound **3** can be enlarged to the $IrRu_4$ complex $IrRu_4(CO)_{12}(\mu_4\text{-}CO)[P(Bu^t)_3]_2(\mu_3\text{-}H)$ (**4**), which contains a type **E** quadruply bridging CO ligand by reaction with $Ru(CO)_5$. Compound **4** reacts with CO to yield the new compound $IrRu_4(CO)_{14}(\mu_4\text{-}\eta^2\text{-}CO)P(Bu^t)_3(\mu\text{-}H)$ (**5**), which contains a type **F** quadruply bridging CO ligand. The results of the studies of these reactions are reported herein.

EXPERIMENTAL SECTION

General Data. Reagent grade solvents were dried by the standard procedures and were freshly distilled prior to use. Infrared spectra were recorded on a Thermo Nicolet Avatar 360 FT-IR spectrophotometer. Room-temperature ^1H NMR and $^{31}P\{^1H\}$ NMR were recorded on a Bruker Avance/DRX 400 NMR spectrometer operating at 400.3 and 162.0 MHz, respectively. Positive/negative ion mass spectra were recorded on a Micromass Q-TOF instrument by using electrospray (ES) ionization or electron impact (EI) ionization. $IrRu_3(CO)_{13}(\mu\text{-}H)$[11] and $Ru(CO)_5$[14] were prepared according to previously reported procedures. $Ru_3(CO)_{12}$ was purchased from Strem, and tri-*tert*-butylphosphine (PBu^t_3) was purchased from Alfa Aesar; both were used without further purification. Product separations were performed by TLC in air on Analtech 0.25 mm silica gel 60 Å F254 glass plates. Due to the small amounts of the products, elemental analyses were not obtained.

Reaction of $IrRu_3(CO)_{13}(\mu\text{-}H)$ with $P(Bu^t)_3$. A 30.0 mg portion (0.0349 mmol) of $IrRu_3(CO)_{13}(\mu\text{-}H)$ was dissolved in 30 mL of methylene chloride solvent in a 100 mL three-neck flask. A 7.5 mg portion of $P(Bu^t)_3$ (0.0371 mmol) was added, and the reaction solution was heated to reflux. The heat was removed after 30 min. An IR spectrum at this time showed that the reaction was not complete. Accordingly, another 1 equiv of $P(Bu^t)_3$ was added and the reaction mixture was stirred overnight at room temperature. The solvent was removed in vacuo, and the products were then isolated by TLC by eluting with a 6/1 hexane/methylene chloride solvent mixture. In order of elution, this yielded 2.5 mg of $Ru_3(CO)_{12}$ (11%), 1.8 mg of $IrRu_3(CO)_{13}(\mu\text{-}H)$ (6.0%, starting material), 5.3 mg of $IrRu_3(CO)_{12}P(Bu^t)_3(\mu\text{-}H)$ (**1**; 15%), 8.6 mg of $IrRu_2(CO)_9[P(Bu^t)_3](\mu\text{-}H)$ (**2**; 29%), and 8.1 mg of $IrRu_3(CO)_{10}[P(Bu^t)_3]_2(\mu_3\text{-}\eta^2\text{-}CO)(\mu\text{-}H)$ (**3**; 19%). Spectral data for **1** are as follows. IR ν_{CO} (cm^{-1} in CH_2Cl_2): 2085 (m), 2045 (vs), 2016 (s), 1993 (m), 1958 (w), 1859 (w). ^1H NMR (CD_2Cl_2, 25 °C, TMS): δ 1.53 (s, 27H, PBu^t_3), −18.39 (d, 1H, J_{P-H} = 6.80 Hz, hydride). $^{31}P\{^1H\}$ NMR (CD_2Cl_2, 25 °C, 85% ortho-H_3PO_4): δ 78.56 (s, 1P, P−Ir). MS (EI+, *m*/*z*): 1036 (M^+), 1008 (M^+−CO). Spectral data for **2** are as follows. IR ν_{CO} (cm^{-1} in CH_2Cl_2): 2087 (s), 2047 (vs), 2014 (s), 2000 (sh), 1986 (m), 1786 (w). ^1H NMR (CD_2Cl_2, 25 °C, TMS): δ 1.49 (d, J_{P-H} = 12.84 Hz, 27H, PBu^t_3), −9.54 (d, 1H, J_{H-P} = 4.96 Hz, hydride). $^{31}P\{^1H\}$ NMR (CD_2Cl_2, 25 °C, 85% ortho-H_3PO_4): δ 98.72 (s, 1P, P−Ir). MS (EI+, *m*/*z*): 852 (M^+). Spectral data for **3** are as follows. IR ν_{CO} (cm^{-1} in CH_2Cl_2): 2061 (s), 2024 (vs), 2011 (s), 1999 (s), 1984 (m), 1976 (m), 1954 (w), 1547 (w). ^1H NMR (CD_2Cl_2, 25 °C): δ 1.54 (s, 27H, PBu^t_3), 1.51 (s, 27H, PBu^t_3), −17.34 (dd, 1H, hydride, $^2J_{H-P}$ = 2.26 Hz, $^3J_{H-P}$ = 3.86 Hz). $^{31}P\{^1H\}$ NMR (CD_2Cl_2, 25 °C, 85% ortho-H_3PO_4): δ 91.22 (s, 1P, P−Ru), 67.46 (s, 1P, P−Ir). MS (ES+, *m*/*z*): 1210 (M^+), 1182 (M^+ − CO).

Reaction of 1 with $P(Bu^t)_3$. A 18.6 mg portion (0.0180 mmol) of $IrRu_3(CO)_{13}(\mu\text{-}H)P(Bu^t)_3$ was dissolved in 30 mL of methylene chloride solvent in a 100 mL three-neck flask. A 5.5 mg portion of $P(Bu^t)_3$ (0.0272 mmol) was added, and the reaction solution was heated to reflux. The heating was stopped after 30 min, and after the removal of solvent in vacuo the products were isolated by TLC by eluting with a 6/1 hexane/methylene chloride solvent mixture. In order of elution, this yielded 0.8 mg of $Ru_3(CO)_{12}$ (7.00%), 4.1 mg of **1** (22.0%, starting material), 2.8 mg of **2** (18.3%), and 8.0 mg of **3** (36.8%).

Synthesis of $IrRu_4(CO)_{12}(\mu_4\text{-}CO)[P(Bu^t)_3]_2(\mu_3\text{-}H)$ (4). A 22.6 mg (portion 0.0187 mmol) of **3** was added to 20 mL of hexane in a 100 mL three-neck flask. $Ru(CO)_5$ (generated by irradiation of $Ru_3(CO)_{12}$ (10.0 mg) in a hexane solution) was then added. After the mixture was heated for 2 h at 68 °C, the solvent was removed in vacuo, and the product was isolated by TLC by using a 3/1 hexane/methylene chloride solvent mixture. A total of 16.9 mg (66% yield) of $IrRu_4(CO)_{12}(\mu_4\text{-}CO)[P(Bu^t)_3]_2(\mu_3\text{-}H)$ (**4**) was obtained. Spectral data for **4** are as follows. IR ν_{CO} (cm^{-1} in CH_2Cl_2): 2065 (s), 2031 (s), 2016 (vs), 1994 (m), 1965 (m), 1934 (w), 1828 (sh), 1780 (w), 1605 (w). ^1H NMR (CD_2Cl_2, 25 °C, TMS): δ 1.65 (s, 27H, PBu^t_3), 1.62 (s, 27H, PBu^t_3), −19.59 (dd, 1H, hydride, $^2J_{P-H}$ = 2.4 Hz, $^3J_{P-H}$ = 1.6 Hz). $^{31}P\{^1H\}$ NMR (CD_2Cl_2, 25 °C, 85% ortho-H_3PO_4): δ 95.79 (s, 1P, P−Ru), 84.63 (s,1P, P−Ir). MS (ES+, *m*/*z*): 1368 (M^+ + H), 1340 (M^+ + H − CO).

Synthesis of $IrRu_4(CO)_{14}P(Bu^t)_3(\mu_4\text{-}\eta^2\text{-}CO)(\mu\text{-}H)$ (5). A 10.0 mg portion (0.0073 mmol) of **4** was added to 10 mL of hexane in a 50 mL three-neck round-bottom flask. CO was then purged continuously through the solution with heating to reflux for 30 min. After cooling, the solvent was removed in vacuo, and the product was then isolated by TLC by using a 4/1 hexane/methylene chloride solvent mixture. This yielded in order of elution 0.5 mg of $Ru_3(CO)_{12}$, 1.6 mg of $IrRu_4(CO)_{14}P(Bu^t)_3(\mu_4\text{-}\eta^2\text{-}CO)(\mu\text{-}H)$ (**5**; 18%), and 1.1 mg of **4** (11%). Spectral data for **5** are as follows. IR ν_{CO} (cm^{-1} in CH_2Cl_2): 2093 (w), 2069 (s), 2056 (vs), 2037 (vs), 2013 (s), 1981 (w). ^1H NMR (CD_2Cl_2, 25 °C, TMS): δ 1.58 (d, J_{P-H} = 12.68 Hz, 27H, PBu^t_3), −17.22 (s, 1H, hydride). $^{31}P\{^1H\}$ NMR (CD_2Cl_2, 25 °C, 85% ortho-H_3PO_4): δ 94.70 (s, 1P, P−Ru). MS (EI+, *m*/*z*): 1193 (M^+ − CO).

Reaction of 5 with CO. A 9.2 mg portion (0.0075 mmol) of **5** was added to 10 mL of hexane in a Parr high-pressure reactor. The reactor was then filled and released with CO five times and finally charged with CO (10 atm); the bomb was placed in an oil bath and heated to 70 °C for 1 h. After the mixture was cooled, the solvent was removed in vacuo, and the product was then isolated by TLC by using a 4/1 hexane/methylene chloride solvent mixture. This yielded in order of elution 3.6 mg of $Ru_3(CO)_{12}$ (56% yield), 1.0 mg of uncharacterized product that decomposed in air, and 2.3 mg (36% yield) of $IrRu_2(CO)_9P(Bu^t)_3(\mu\text{-}H)$ (**2**).

Crystallographic Analyses. Black crystals of **1**, green crystals of **2**, red crystals of **3**, black crystals of **4**, and red crystals of **5** suitable for X-ray diffraction analyses were all obtained by slow evaporation of solvent from solutions in methylene chloride/hexane solvent mixtures at −25 °C. X-ray intensity data were measured on a Bruker SMART APEX CCD-based diffractometer by using Mo Kα radiation (λ = 0.71073 Å). The raw data frames were integrated with the SAINT+

program by using a narrow-frame integration algorithm.[15] Correction for Lorentz and polarization effects were also applied using SAINT+. All structures were solved by a combination of direct methods and difference Fourier syntheses and were refined by full-matrix least squares on F^2 by using the SHELXTL software package.[16] See the Supporting Information for additional details.

Computational Details. Density functional theory (DFT) calculations were performed with the Amsterdam Density Functional (ADF) suite of programs[17] by using the PBEsol functional[18] with scalar relativistic correction and valence quadruple-ζ + 4 polarization, relativistically optimized (QZ4P) basis sets for iridium and ruthenium, and valence triple-ζ + 2 polarization function (TZ2P) basis sets for the phosphorus, carbon, oxygen, and hydrogen atoms with no frozen cores. The molecular orbitals for **2**–**5** and their energies were determined by geometry optimized calculations that were initiated with the structures as determined from the crystal structure analyses.

RESULTS AND DISCUSSION

Three compounds were obtained from the reaction of $IrRu_3(CO)_{13}(\mu_3\text{-H})$ with $P(Bu^t)_3$ in hexane solution at reflux for 30 min. These have been identified as $IrRu_3(CO)_{12}P(Bu^t)_3(\mu\text{-H})$ (**1**; 15% yield), $IrRu_2(CO)_9[P(Bu^t)_3](\mu\text{-H})$ (**2**; 29% yield), and $IrRu_3(CO)_{10}(\mu_3\text{-}\eta^2\text{-CO})[P(Bu^t)_3]_2(\mu\text{-H})$ (**3**; 19% yield). All three products were characterized by a combination of IR, ^{1}H NMR, and mass spectra and single-crystal X-ray diffraction analyses. An ORTEP diagram of the molecular structure of **1** is shown in Figure 1.

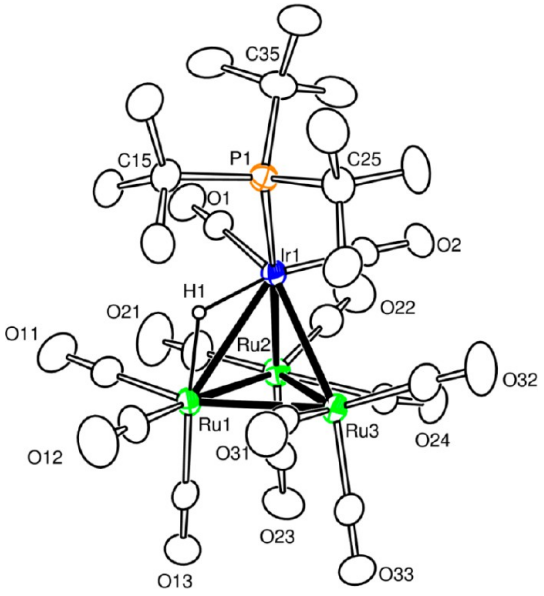

Figure 1. ORTEP diagram of the molecular structure of $IrRu_3(CO)_{12}P(Bu^t)_3(\mu\text{-H})$ (**1**) showing thermal ellipsoids at the 30% probability level. Selected interatomic bond distances (Å) are as follows: Ir(1)–Ru(1) = 2.9115(5), Ir(1)–Ru(2) = 2.7750(5), Ir(1)–Ru(3) = 2.8257(5), Ru(1)–Ru(2) = 2.7801(7), Ru(1)–Ru(3) = 2.7735(6), Ir(1)–H(1) = 1.70(5), Ru(1)–H(1) = 1.76(5), Ru(2)–Ru(3) = 2.7837(7), Ir(1)–P(1) = 2.4825(15).

Compound **1** is simply a $P(Bu^t)_3$ substitution derivative of its parent $IrRu_3(CO)_{13}(\mu_3\text{-H})$.[12] Compound **1** contains a closed tetrahedral cluster of four metal atoms, one of Ir and three of Ru. There is one hydrido ligand in **1** that bridges the Ir(1)–Ru(1) bond. The Ir(1)–Ru(1) bond distance (2.9115(5) Å) is significantly longer than the two other Ir–Ru bonds (Ir(1)–Ru(2) = 2.7750(5) Å and Ir(1)–Ru(3) = 2.8257(5) Å). It is well-known that bridging hydrido ligands increase the length of the metal–metal bonds that they bridge.[19] The hydrido ligand in **1** exhibits the expected high-field resonance shift in the ^{1}H NMR spectrum, −18.39 ppm with small coupling, $^2J_{H-P}$ = 6.80 Hz, to the phosphorus atom of the proximate $P(Bu^t)_3$ ligand. The phosphine ligand is coordinated to the iridium atom (Ir(1)–P(1) = 2.4825(15) Å). The cluster contains a total of 60 valence electrons and is thus electronically saturated; i.e., all metal atoms formally have 18-electron configurations.

An ORTEP diagram of the molecular structure of **2** is shown in Figure 2. Compound **2** contains only three metal atoms, one

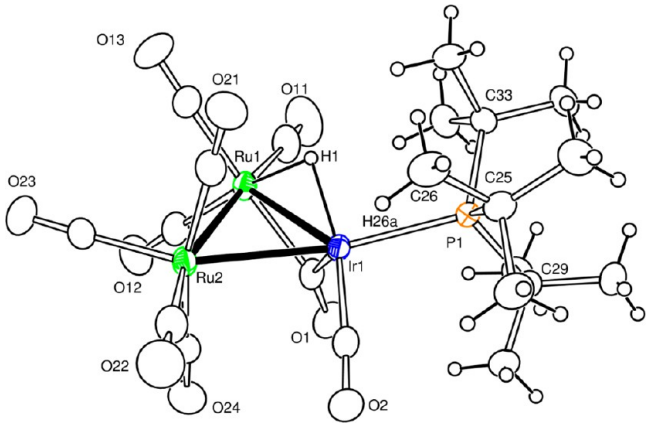

Figure 2. ORTEP diagram of molecular structure of $IrRu_2(CO)_9P(Bu^t)_3(\mu\text{-H})$ (**2**) showing thermal ellipsoids at the 30% probability level. Selected interatomic bond distances (Å) are as follows: Ir(1)–Ru(1) = 2.7570(3), Ir(1)–Ru(2) = 2.7659(3), Ru(1)–Ru(2) = 2.8243(4), Ir(1)–P(1) = 2.3863(9), Ir(1)–C(1) = 2.013(4), Ru(1)–C(1) = 2.089(4), Ir(1)–H(1) = 1.83(4), Ru(1)–H(1) = 1.77(4), Ir(1)···C(26) = 3.310(4), Ir(1)···H(26a) = 2.71.

of Ir and two of Ru. They are arranged in a triangle. The Ir–Ru bonds are short but are not exceptionally short (Ir(1)–Ru(1) = 2.7570(3) Å, Ir(1)–Ru(2) = 2.7659(3) Å, and Ru(1)–Ru(2) = 2.8243(4) Å). There is one hydrido ligand that bridges the Ir(1)–Ru(1) bond (Ir(1)–H(1) = 1.83(4) Å and Ru(1)–H(1) = 1.77(4) Å). The hydride ligand exhibits a high-field resonance at −9.54 ppm with coupling to the neighboring phosphorus atom, $^2J_{P-H}$ = 4.96 Hz, but the shift is not nearly as high as that found in **1** or the other complexes **3**–**5**. This may be related to the electronic unsaturation found in **2** (see below).[20] The phosphine ligand is coordinated to the iridium atom (Ir(1)–P(1) = 2.3863(9) Å). There are eight terminally coordinated carbonyl ligands, and there is one CO (C(1)–O(1)) ligand that bridges the Ir(1)–Ru(1) bond. Overall, compound **2** contains a total of 46 valence electrons and is thus electron deficient by the amount of two electrons. The deficiency appears to be located primarily at the iridium atom, which formally contains only 16 valence electrons. Indeed, there appears to be a vacant coordination site on Ir(1) that lies approximately trans to the bond to the bridging CO ligand. This site is protected in part by one of the methyl groups (C26) on one of the *tert*-butyl groups of the bulky $P(Bu^t)_3$ ligand, and the distance to C(26) and one of the hydrogen atoms (H(26a)) on that methyl group is notably short (Ir(1)···C(26) = 3.310(4) Å, Ir(1)···H(26a) = 2.71 Å). This could be interpreted as a weak agostic C–H interaction to the Ir atom. A similar arrangement was found at the unsaturated vacant site in the complex $Re_2(CO)_6[P(Bu^t)_3][\mu\text{-}P(Bu^t)_2](\mu\text{-H})$.[20] Indeed,

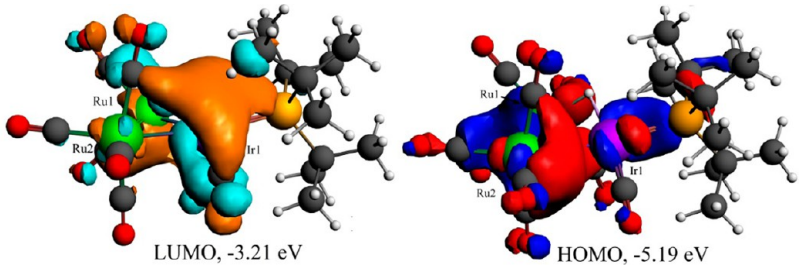

Figure 3. ADF MO diagrams of the LUMO (left) and HOMO (right) for compound **2**. A large component of the LUMO shown in gold lies in the proximity of the vacant coordination site on the iridium atom. Color scheme: violet, Ir; green, Ru; red, O; gray, C. The isovalue is 0.03.

the position of this methyl group prevents the addition of CO to the Ir atom at this site in **2**.

In order to examine the electronic structure of **2** further, DFT molecular orbital calculations were performed by using the PBEsol functional in the ADF program library. A diagram of the LUMO of **2** is shown in Figure 3 and is in accordance with the conventional electron counting procedures; the LUMO shows a large component which lies at approximately the same location as the vacant coordination site on the iridium atom. Süss-Fink reported two related $IrRu_2$ cluster complexes, $HRu_2Ir(CO)_5(dppm)_3$ and $HRu_2Ir(CO)_6(PCy_3)_3$.[21] The former complex contains 48 valence electrons, but the latter, which contains three bulky PCy_3 ligands (Cy = cyclohexyl), contains only 44 valence electrons.

An ORTEP diagram of the molecular structure of **3** is shown in Figure 4. Compound **3** contains four metal atoms, one of Ir

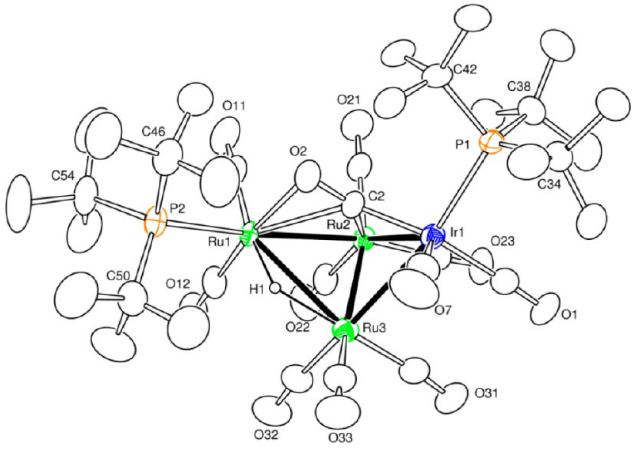

Figure 4. ORTEP diagram of molecular structure of $IrRu_3(CO)_{10}(\mu_3$-η^2-CO)$[P(Bu^t)_3]_2(\mu$-H) (**3**) showing thermal ellipsoids at the 30% probability level. Selected interatomic bond distances (Å) are as follows: Ir(1)−Ru(2) = 2.8722(8), Ir(1)−Ru(3) = 2.8783(9), Ir(1)−P(1) = 2.470(2), Ir(1)−C(2) = 1.917(9), Ru(1)−Ru(2) = 2.8563(9), Ru(1)−Ru(3) = 3.0574(10), Ru(1)−P(2) = 2.496(2), Ru(1)−C(2) = 2.476(10), Ru(1)−O(2) = 2.168(8), Ru(1)−H(1) = 1.627, Ru(2)−Ru(3) = 2.7311(11), Ru(2)−C(2) = 2.150(10), Ru(3)−H(1) = 1.829, C(2)−O(2) = 1.250(11).

and three of Ru. They are arranged in the form of a butterfly tetrahedron. There are two $P(Bu^t)_3$ ligands, one on Ir(1) and the other on Ru(1), and these two metal atoms occupy the less crowded "wingtip" positions of the butterfly tetrahedron. The metal−metal bond distances are fairly normal (Ir(1)−Ru(2) = 2.8722(8) Å, Ir(1)−Ru(3) = 2.8783(9) Å, Ir(1)−P(1) = 2.470(2) Å, Ir(1)−C(2) = 1.917(9) Å, Ru(1)−Ru(2) = 2.8563(9) Å, Ru(2)−Ru(3) = 2.7311(11) Å), except for Ru(1)−Ru(3), which is unusually long at 3.0574(10) Å. The long Ru(1)−Ru(3) bond can be attributed to the presence of a hydrido ligand which bridges that bond.[19] The hydrido ligand exhibits a high-field resonance shift (−17.34 ppm) with coupling to the two phosphorus atoms ($^2J_{H-P}$ = 2.26 Hz and $^3J_{H-P}$ = 3.86 Hz).

The most interesting ligand in **3** is a η^2 triply bridging CO ligand (C(2)−O(2)) of the type **D**. The carbon atom is bonded to three of the metal atoms. The Ru(1)−C(2) bond distance (2.476(10) Å) is significantly longer than the other two bonds to C(2) (Ir(1)−C(2) = 1.917(9) Å and Ru(2)−C(2) = 2.150(10) Å) but seems to contain important bonding interactions (see below). The oxygen atom is bonded to Ru(1) (Ru(1)−O(2) = 2.168(8) Å), and as a result, the CO bond distance is long (C(2)−O(2)= 1.250(11) Å) in comparison to that of the terminally coordinated CO ligands (average 1.14(2) Å).

In order to understand the nature of the coordination of the triply bridging CO ligand better, a geometry-optimized DFT molecular orbital analysis of compound **3** was performed. Selected MOs that show the bonding of the bridging CO ligand to the metal atoms are shown in Figure 5. The HOMO and HOMO-2 show π back-bonding between the three metal atoms and one of the π^* molecular orbitals of the CO ligand. HOMO-53 and HOMO-93 show donation of electrons via the filled π-bonding orbitals on the CO ligand to the same metal atoms.

In addition, HOMO-103 shows bonding interactions of the CO σ-bonding orbital, $5A_1$, frequently referred to as the "lone" pair of electrons on the carbon atom to the metal atoms Ru(2) and Ir(1). PBEsol DFT MOs for the uncoordinated CO molecule are available (see the Supporting Information). Assuming the bridging CO ligand serves as a four-electron donor, the metal cluster in **3** contains a total of 62 valence electrons, which is exactly the number expected for an electron-precise cluster of four metal atoms having five metal−metal bonds: i.e., each of the metal atoms formally achieves an 18-electron configuration.

Compound **3** was found to react with $Ru(CO)_5$ to give the higher nuclearity cluster complex $IrRu_4(CO)_{12}(\mu_4$-CO)$[P(Bu^t)_3]_2(\mu_3$-H) (**4**) in 66% yield. An ORTEP diagram of the molecular structure of **4** is shown in Figure 6.

Compound **4** contains five metal atoms, one of Ir and four of Ru. The metal atoms are arranged in the form of an iridium-capped butterfly tetrahedron of four ruthenium atoms. There are two $P(Bu^t)_3$ ligands, one on the iridium atom Ir(1) and the other on Ru(2). The Ir−Ru bond distances are normal (Ir(1)−Ru(1) = 2.8440(4) Å, Ir(1)−Ru(3) = 2.8061(4) Å, and Ir(1)−Ru(4) = 2.8353(4) Å). The Ru−Ru distances are also normal (Ru(1)−Ru(2) = 2.9081(5) Å, Ru(1)−Ru(3) = 2.9128(5) Å, Ru(1)−Ru(4) = 2.7816(5) Å, Ru(2)−Ru(3) = 2.8958(5) Å,

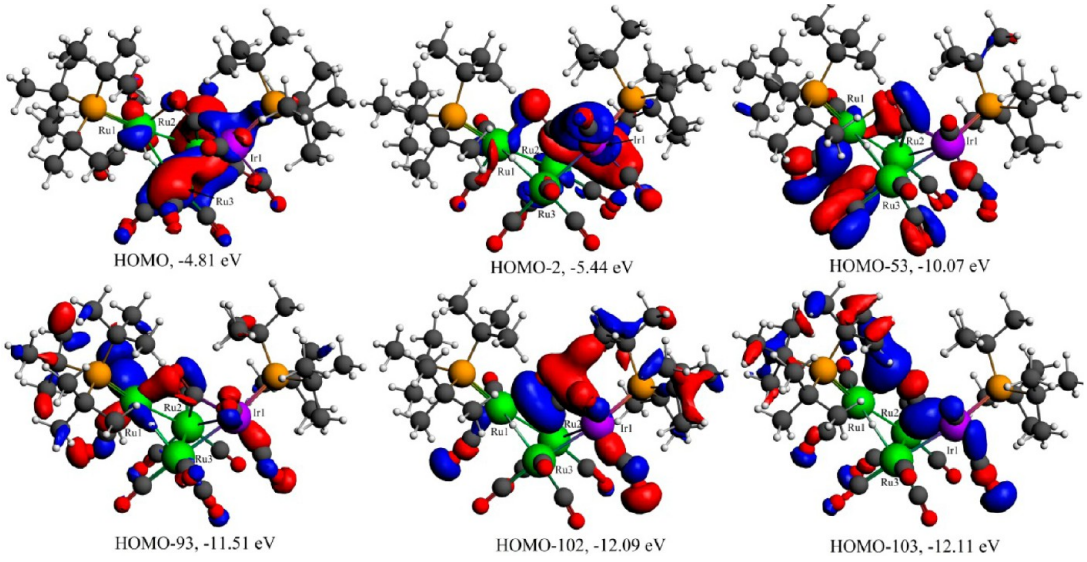

Figure 5. Selected ADF MO diagrams for compound **3** showing the bonding of the bridging CO ligand to the metal atoms Color scheme: violet, Ir; green, Ru; red, O; gray, C. The isovalue is 0.03.

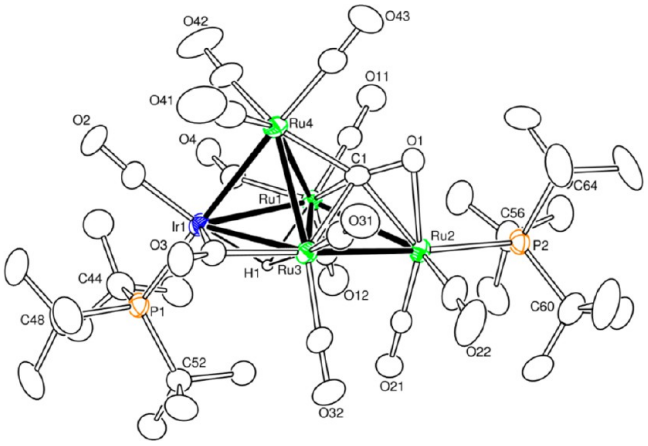

Figure 6. ORTEP diagram of molecular structure of $IrRu_4(CO)_{12}[P(Bu^t)_3]_2(\mu_4\text{-}\eta^2\text{-}CO)(\mu_3\text{-}H)$ (**4**), showing thermal ellipsoids at the 30% probability level. Selected interatomic bond distances (Å) are as follows: Ir(1)−Ru(1) = 2.8440(4), Ir(1)−Ru(3) = 2.8061(4), Ir(1)−Ru(4) = 2.8353(4), Ir(1)−P(1) = 2.4582(12), Ir(1)−H(1) = 1.78(4), Ru(1)−Ru(2) = 2.9081(5), Ru(1)−Ru(3) = 2.9128(5), Ru(1)−Ru(4) = 2.7816(5), Ru(1)−C(1) = 2.164(4), Ru(1)−H(1) = 1.99(4), Ru(2)−Ru(3) = 2.8958(5), Ru(2)−P(2) = 2.4932(12), Ru(2)−C(1) = 2.242(4), Ru(2)−O(1) = 2.139(3), Ru(3)−Ru(4) = 2.8204(5), Ru(3)−H(1) = 1.96(4), Ru(3)−C(1) = 2.156(4), Ru(4)−C(1) = 2.083(5), C(1)−O(1) = 1.256(5).

and Ru(3)−Ru(4) = 2.8204(5) Å). The hydrido ligand, located and refined in the structural analysis, was found to be a triply bridging ligand across the Ir(1)−Ru(1)−Ru(3) triangle (Ir(1)−H(1) = 1.78(4) Å, Ru(1)−H(1) = 1.99(4) Å, and Ru(3)−H(1) = 1.96(4) Å). It exhibits a very high field resonance shift in the ^{1}H NMR spectrum (−19.47 ppm) with coupling to the two phosphorus atoms ($^2J_{P-H}$ = 2.4 Hz and $^3J_{P-H}$ = 1.6 Hz). Compound **4** contains a η^2-quadruply bridging CO ligand (C(1)−O(1)) of the type **E**. The carbon atom is bonded to all four ruthenium atoms (Ru(1)−C(1) = 2.164(4) Å, Ru(2)−C(1) = 2.242(4) Å, Ru(3)−C(1) = 2.156(4) Å, and Ru(4)−C(1) = 2.083(5) Å0. The oxygen atom is bonded only to Ru(2) (Ru(2)−O(1) = 2.139(3) Å). As found in **3**, the CO bond distance is also long (C(1)−O(1) = 1.256(15) Å).

DFT molecular orbital calculations have revealed the nature of the coordination of the quaduply bridging CO ligand to the four ruthenium atoms. Selected MOs that show the bonding of the η^2 quadruply bridging CO ligand to the four metal atoms in **4** are shown in Figure 7. HOMO-1 and HOMO-13 show η^2 π back-bonding from the metal atoms into one of the π*-orbitals of the CO ligand at both the carbon and oxygen atoms. The HOMO-60 and HOMO-61 show π-donation from the filled π orbitals on the CO ligand to the metal atoms. HOMO-110 and HOMO-111 show σ donation from the CO ligand σ bond to the metal atoms, principally to Ru(2). HOMO-112 shows π donation from the filled π orbitals on the CO ligand to the metal atoms, and HOMO-132 shows a strong σ donation from the CO carbon atom to the Ru3 triangle (Ru(1), Ru(3), and Ru(4)). In this way the quadruply bridging CO ligand is able to serve formally as a four-electron donor and the cluster thus contains a total of 74 valence electrons, which is exactly the number expected for an electron-precise edge-bridged tetrahedron or a capped butterfly tetrahedron: that is, all of the metal atoms achieve 18-electron configurations.[22]

When compound **4** was treated with CO (1 atm) in a hexane solution at reflux for 30 min, the new compound $IrRu_4(CO)_{14}P(Bu^t)_3(\mu_4\text{-}\eta^2\text{-}CO)(\mu\text{-}H)$ (**5**) was obtained in 18% yield. Compound **5** was characterized crystallographically, and an ORTEP diagram of its molecular structure is shown in Figure 8. Like **4**, compound **5** also contains five metal atoms, one of Ir and four of Ru. The metal atoms are arranged in the form of a spiked tetrahedron. The iridium atom is contained in the tetrahedral portion of the cluster (Ir(1)−Ru(2) = 2.7831(5) Å, Ir(1)−Ru(3) = 2.7295(6) Å, and Ir(1)−Ru(4) = 2.7814(5) Å). Ru(1) is the "spike" that is bonded only to the iridium atom (Ir(1)−Ru(1) = 2.8215(5) Å). There is only one $P(Bu^t)_3$ ligand in **5**, and it is coordinated to the ruthenium atom Ru(1) (Ru(1)−P(1) = 2.5205(16) Å). There is one hydrido ligand H(1) that bridges the Ru(2)−Ru(3) bond (Ru(2)−H(1) = 1.79(6) Å and Ru(3)−H(1) = 1.74(5) Å), and as a result that metal−metal bond is significantly longer (Ru(2)−Ru(3) = 2.9569(7) Å) than the other two (Ru(2)−

dx.doi.org/10.1021/om400722z | Organometallics 2013, 32, 5171−5179

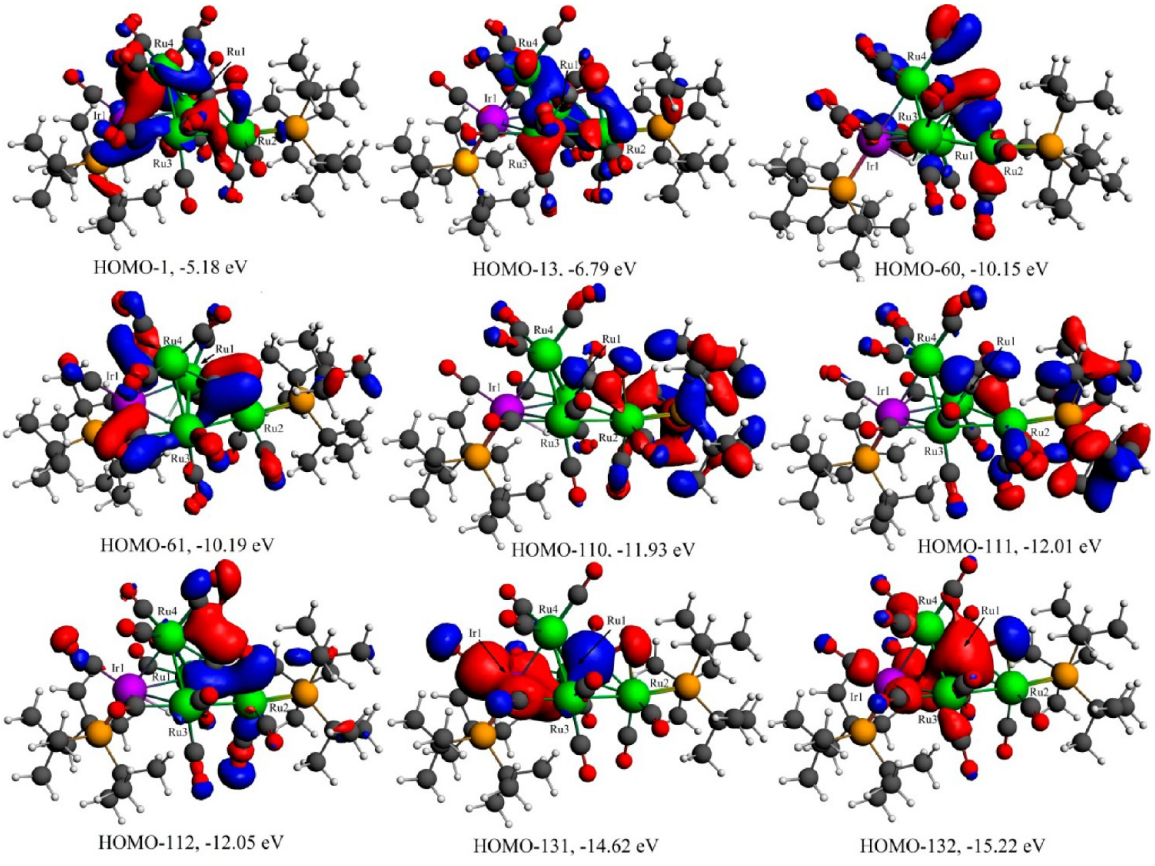

Figure 7. Selected ADF MO diagrams with energies for compound **4** showing the bonding of the quadruply bridging CO ligand to the metal atoms of the cluster. Color scheme: violet, Ir; green, Ru; red, O; gray, C. The isovalue is 0.03.

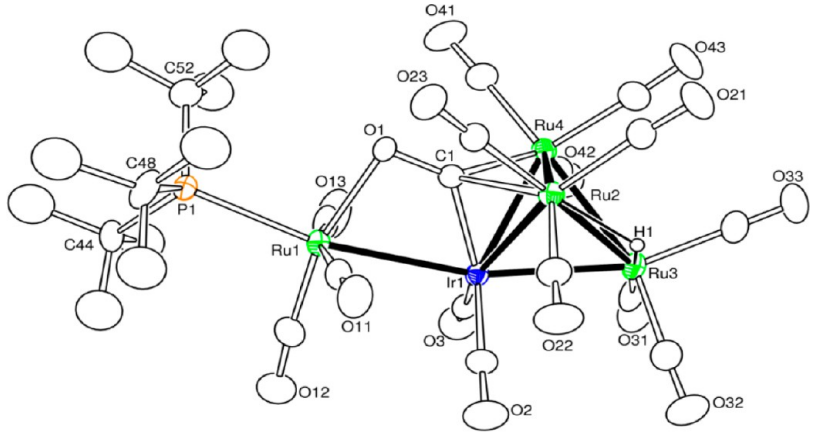

Figure 8. ORTEP diagram of the molecular structure of $IrRu_4(CO)_{14}P(Bu^t)_3(\mu_4\text{-}\eta^2\text{-}CO)(\mu\text{-}H)$ (**5**), showing thermal ellipsoids at the 30% probability level. Selected interatomic bond distances (Å) are as follows: Ir(1)−Ru(1) = 2.8215(5), Ir(1)−Ru(2) = 2.7831(5), Ir(1)−Ru(3) = 2.7295(6), Ir(1)−Ru(4) = 2.7814(5), Ir(1)−C(1) = 2.009(6), Ru(1)−P(1) = 2.5205(16), Ru(1)−O(1) = 2.159(4), Ru(1)−C(1) = 2.619(6), Ru(2)−Ru(3) = 2.9569(7), Ru(2)−Ru(4) = 2.7921(7), Ru(2)−C(1) = 2.287(6), Ru(2)−H(1) = 1.79(6), Ru(3)−Ru(4) = 2.7940(7), Ru(3)−H(1) = 1.74(5), Ru(4)−C(1) = 2.036(6), C(1)−O(1) = 1.269(7).

Ru(4) = 2.7921(7) Å and Ru(3)−Ru(4) = 2.7940(7) Å).[19] The hydrido ligand exhibits a high-field resonance shift in the ^{1}H NMR spectrum (−17.22 ppm). No coupling was observed to the remotely positioned phosphorus atom of the $P(Bu^t)_3$ ligand. An η^2 quadruply bridging carbonyl ligand (C(1)−O(1)) of the general form **F** is coordinated to three metal atoms Ir(1), Ru(2), and Ru(4) by its carbon atom. Two of the M−C bonds are quite short (Ir(1)−C(1) = 2.009(6) Å and Ru(4)−C(1) = 2.036(6) Å); the third bond Ru(2)−C(1) which lies trans to the bridging hydrido ligand (see below) is much longer at 2.287(6) Å. The oxygen atom is coordinated only to Ru(1) (Ru(1)−O(1) = 2.159(4) Å). The Ru(1)−C(1) distance at 2.619(6) Å is believed to be largely nonbonding. As found in **2** and **3**, the CO bond distance is also long (C(1)−O(1) = 1.269(7) Å). Compound **5** contains a total of 76 valence electrons, which is precisely the number expected for a spiked-tetrahedral cluster of five metal atoms.[22] Compound **5**

Scheme 3. Proposed Transformation of 4 to 5 under a CO Atmosphere

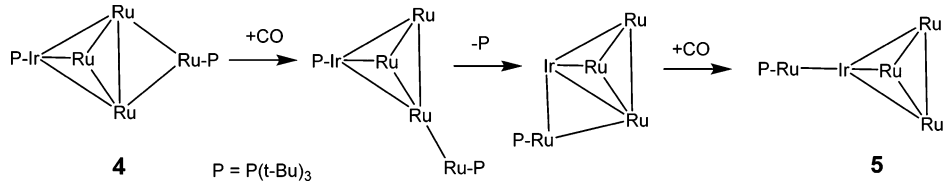

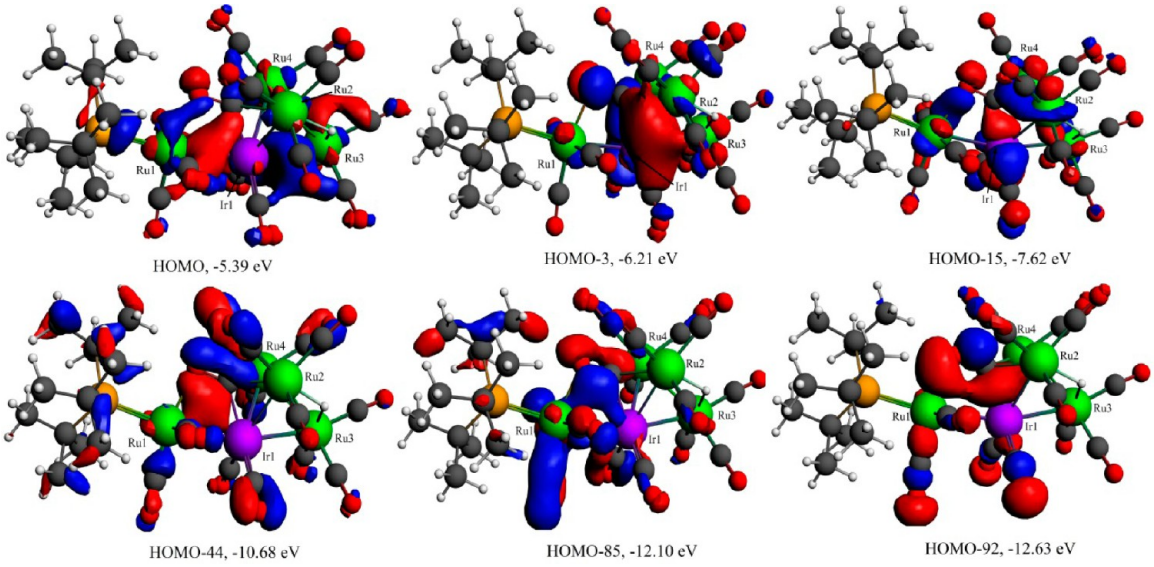

Figure 9. ADF MO diagrams with energies for compound **5** showing the bonding of the quadruply bridging CO ligand to the metal atoms of the cluster. Color scheme: violet, Ir; green, Ru; red, O; gray, C. The isovalue is 0.03.

was formed by the loss of one of the $P(Bu^t)_3$ ligands from **4** and the addition of two CO ligands.

Thus, in the conversion from **4** to **5**, the number of ligands was increased by one and accordingly the number of metal–metal bonds was decreased by one. Assuming that the $P(Bu^t)_3$ ligand is bonded to the same Ru atom in **5** that it was in **4**, then that Ru grouping must make a shift from the Ru atoms to the Ir atom. This can be achieved by a series of ligand additions and eliminations, as shown schematically in Scheme 3, where ligand additions lead to cleavage of metal–metal bonds and ligand eliminations lead to the formation of metal–metal bonds.

In order to obtain a better understanding of the bonding of the η^2 quaduply bridging CO ligand to the four metal atoms in **5**, DFT molecular orbital calculations were performed. Selected MOs that show the bonding of the bridging CO ligand to the four metal atoms in **5** are shown in Figure 9. HOMO and HOMO-15 show η^2 π back-bonding from Ru(1) and Ir(1) both to the carbon and to the oxygen atom of the CO ligand via one of the CO π^* orbitals. HOMO-3 shows η^1 π back-bonding to the other CO π^* orbital via the carbon atom alone. Recalling that the η^2 quaduply bridging CO ligand serves formally as a four-electron donor, a search of the low-lying orbitals did provide the expected evidence for electron-donating interactions to support this model. In particular, HOMO-44 and HOMO-85 show η^2 π donations to the metal atoms from each of the filled CO π-bonding orbitals and HOMO-92 shows donation from the CO σ-orbital $5A_1$ that is frequently referred to as the lone pair or electrons on the carbon atom. The CO portion of HOMO-92 is distorted from its classical linear form because of its unsymmetrical bonding to the metal atoms. DFT MOs for the uncoordinated CO molecule are available (see the Supporting Information).

When compound **5** was treated with CO at 70 °C/10 atm for 1 h, it was converted to **2** in 36% yield by removal of two of the Ru groups. $Ru_3(CO)_{12}$ was isolated as a coproduct in 56% yield.

SUMMARY

A summary of the results of this study are shown in Scheme 4.

The principal products formed by the reaction of $IrRu_3(CO)_{13}(\mu_3\text{-H})$ with $P(Bu^t)_3$ are the closed and open $IrRu_3$ cluster complexes **1** and **3**. Complex **2** is a lower nuclearity cluster complex formed by the loss of one Ru grouping and is particularly interesting because it is electronically unsaturated. Compound **4** is a higher nuclearity species obtained from **3** by the addition of an Ru grouping from $Ru(CO)_5$. Compound **5** was obtained from **4** by treatment with CO accompanied by a rearrangement of the metal atoms. Compounds **3**–**5** all contain an η^2-bridging CO ligand which stabilizes the open structures of the clusters.

CONCLUSIONS

In previous studies we showed that the introduction of the bulky $P(Bu^t)_3$ ligand into polynuclear transition-metal carbonyl complexes can induce electronic unsaturation around the metal atoms via ligand deficiencies.[20,23]This is also evident in the electronically unsaturated compound **2** described in this work. Compounds **3**–**5** are formally electron precise, but all of them have a bridging CO ligand that serves as a four-electron donor. The multielectron coordination of the η^2-bridging CO ligands in the various coordination environments has been examined by DFT computational analysis and has been shown to involve

Scheme 4. Reaction of $HIrRu_3(CO)_{13}$ with PBu^t_3 and Transformations of the Various Cluster Products via the Medium of the η^2-Bridging Carbonyl Ligand

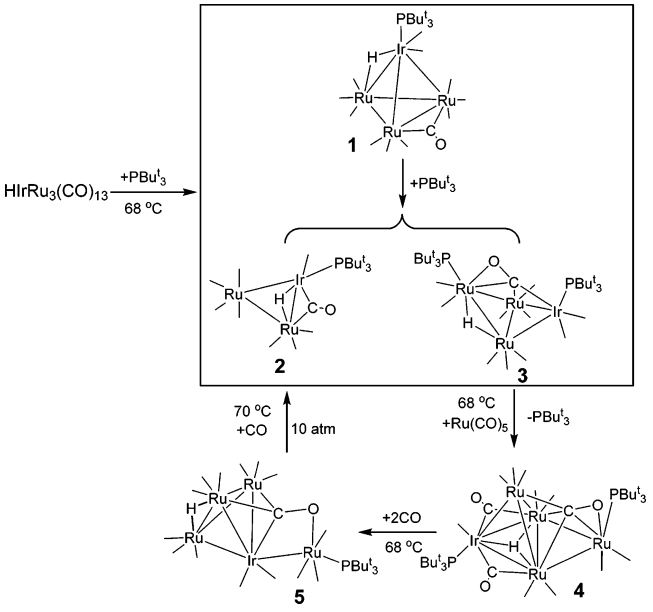

a combination of σ- and π-donation effects. If the η^2-bridging CO ligand in **3**–**5** was a terminally coordinated two-electron donor, then all of these complexes would also be electronically unsaturated. We feel that these higher nuclearity metal complexes have adopted the observed structures with four-electron bridging CO ligands in order to eliminate the potential problem of electronic unsaturation. One might ask why does not the molecule simply add another CO ligand and then have two terminally coordinated two-electron-donating CO ligands instead of one four-electron η^2-bridging CO ligand. The answer might simply be steric effects. Two terminally coordinated CO ligands will almost certainly occupy more space than one η^2-bridging CO ligand. Although two atoms are coordinated to the metal atoms in both cases, for the η^2-bridging CO, the two atoms C and O are bonded to each other at a short distance, approximately 1.25 Å, and thus would occupy much less space in the coordination sphere of the metal atoms than two nonbonded carbon atoms from two terminally coordinated CO ligands.

■ ASSOCIATED CONTENT

Ⓢ Supporting Information

Text and tables giving details of the computational analyses for **2**–**5** and CIF files and tables of selected bond distances and angles for the structural analyses of **1**–**5**. This material is available free of charge via the Internet at http://pubs.acs.org.

■ AUTHOR INFORMATION

Corresponding Author

*E-mail for R.D.A.: Adamsrd@mailbox.sc.edu.

Notes

The authors declare no competing financial interest.

■ ACKNOWLEDGMENTS

This research was supported by the following grants from the National Science Foundation: CHE-1111496 and CHE-1048629.

■ REFERENCES

(1) (a) Niibayashi, S.; Mitsui, K.; Matsubara, K.; Nagashima, H. *Organometallics* **2003**, *22*, 4885–4892. (b) Stutte, B.; Batzel, V.; Boese, R.; Schmid, G. *Chem. Ber.* **1978**, *111*, 1603–1618. (c) Schmid, G.; Stutte, B.; Boese, R. *Chem. Ber.* **1978**, *111*, 1239–1245. (d) Gambarotta, S.; Stella, S.; Floriani, C.; Chiesi-Villa, A.; Guastini, C. *Angew. Chem., Int. Ed.* **1986**, *25*, 254–255. (e) Fachinetti, G.; Fochi, G.; Funaioli, T.; Zanazzi, P. F. *Angew. Chem., Int. Ed.* **1987**, *26*, 680–681.

(2) (a) Field, J. S.; Haines, R. J.; Jay, J. A. *J. Organomet. Chem.* **1989**, *377*, C35–C39. (b) Adams, R. D.; Li, Z.; Lii, J.-C.; Wu, W. *Organometallics* **1992**, *11*, 4001–4009.

(3) (a) Adams, R. D.; Babin, J. E.; Tasi, M. *Inorg. Chem.* **1988**, *27*, 2618–2625. (b) Cabeza, J. A.; del Rio, I.; Miguel, D.; Pérez-Carreno, E.; Sánchez-Vega, M. G. *Dalton Trans.* **2008**, 1937–1942. (c) Yun, C.; Su, C. J.; Tseng, W. C.; Peng, S. M.; Lee, G. H. *J. Cluster Sci.* **1997**, *8*, 507–519. (d) Yun, C.; Su, C. J.; Peng, S. M.; Lee, G. H. *J. Am. Chem. Soc.* **1997**, *119*, 11114–11115. (e) Su, P. C.; Chi, Y.; Su, C. J.; Peng, S. M.; Lee, G. H. *Organometallics* **1997**, *16*, 1870–1874. (f) Adams, R. D.; Alexander, M. S.; Arafa, I.; Wu, W. *Inorg. Chem.* **1991**, *30*, 4717–4723. (g) Gibson, C. P.; Dahl, L. F. *Organometallics* **1988**, *7*, 535–543. (h) Chi, Y.; Chuang, S. H.; Liu, L. K.; Wen, Y. S. *Organometallics* **1991**, *10*, 2485–2492. (i) Notaras, E. G. A.; Lucas, N. T.; Humphrey, M. G. *J. Organomet. Chem.* **2001**, *631*, 139–142. (j) Nahar, S.; Davies, J. E.; Shields, G. P.; Raithby, P. R. *J. Cluster Sci.* **2010**, *21*, 379–396. (k) Femoni, C.; Iapalucci, M. C.; Longoni, G.; Zacchini, S. *Dalton Trans.* **2011**, *40*, 8685–8694. (l) Horwitz, C. P.; Holt, E. M.; Brock, C. P.; Shriver, D. F. *J. Am. Chem. Soc.* **1985**, *107*, 8136–8146. (m) Bailey, P. J.; Duer, M. J.; Johnson, B. F. G.; Lewis, J.; Conole, G.; McPartlin, M.; Powell, H. R.; Anson, C. E. *J. Organomet. Chem.* **1990**, *383*, 441–461.

(4) (a) Brun, P.; Dawkins, G. M.; Green, M.; Miles, A. D.; Orpen, A. G.; Stone, F. G. A. *Chem. Commun.* **1982**, 926–927. (b) Johnson, B. F. G.; Lewis, J.; McPartlin, M.; Pearsall, M.-A.; Sironi, A. *Chem. Commun.* **1984**, 1089–1090. (c) Leung, K. S.-Y. *Inorg. Chem. Commun.* **1999**, *2*, 498–502. (d) Leung, K. S.-Y.; Wong, W. T. *J. Chem. Soc., Dalton Trans.* **1997**, 4357–4360. (e) Chisholm, M. H.; Folting, K.; Hampden-Smith, M. J.; Hammond, C. E. *J. Am. Chem. Soc.* **1989**, *111*, 7283–7285.

(5) (a) Herrmann, W. A.; Ziegler, M. L.; Windenhammer, K.; Biersack, H. *Angew. Chem., Int. Ed. Engl.* **1979**, *18*, 960–962. (b) Herrmann, W. A.; Biersack, H.; Ziegler, M. L.; Windenhammer, K.; Siegel, R.; Rehder, D. *J. Am. Chem. Soc.* **1981**, *103*, 1692–1699.

(6) (a) Bailey, P. J.; Johnson, B. F. G.; Lewis, J. *Inorg. Chim. Acta* **1994**, *227*, 197–200. (b) Martin, C. M.; Dyson, P. J.; Ingham, S. L.; Johnson, B. F. G.; Blake, A. J. *J. Chem. Soc., Dalton Trans.* **1995**, 2741–2748. (c) Anson, C. E.; Bailey, P. J.; Conole, G.; Johnson, B. F. G.; Lewis, J.; McPartlin, M.; Powell, H. R. *J. Chem. Soc., Chem. Commun.* **1989**, 442–444. (d) Shriver, D. F.; Sailor, M. J. *Acc. Chem. Res.* **1988**, *21*, 374–379.

(7) (a) Corrigan, J. F.; Doherty, S.; Taylor, N. J.; Carty, A. J. *Organometallics* **1993**, *12*, 993–995. (b) Chi, Y.; Su, C. J.; Farrugia, L. J.; Peng, S. M.; Lee, G. H. *Organometallics* **1994**, *13*, 4167–4169.

(8) Van Santen, R. A.; Neurock, M. In *Molecular Heterogeneous Catalysis. A Conceptual and Computational Approach*; Wiley-VCH: Weinheim, Germany, 2006; pp 121–125.

(9) (a) Muetterties, E. L.; Stein, J. *Chem. Rev.* **1979**, *79*, 479–490. (b) Herrmann, W. A. *Angew. Chem., Int. Ed. Engl.* **1982**, *21*, 117–130.

(10) (a) Adams, R. D. *J. Organomet. Chem.* **2000**, *600*, 1–6. (b) Adams, R. D.; Li, Z.; Swepston, P.; Wu, W.; Yamamoto, J. *J. Am. Chem. Soc.* **1992**, *114*, 10657–10658. (c) Adams, R. D.; Barnard, T. S.; Li, Z.; Wu, W.; Yamamoto, J. *J. Am. Chem. Soc.* **1994**, *116*, 9103–9113. (d) Adams, R. D.; Barnard, T. S. *Organometallics* **1998**, *17*, 2567–2573. (e) Pignolet, L. H.; Aubart, M. A.; Craighead, K. L.; Gould, R. A. T.; Krogstad, D. A.; Wiley, J. S. *Coord. Chem. Rev.* **1995**, *143*, 219–263.

(11) Ferrand, V.; Süss-Fink, G.; Neels, A.; Stoeckli-Evans, H. *J. Chem. Soc., Dalton Trans.* **1998**, 3825–3831.

(12) Süss-Fink, G.; Haak, S.; Neels, A.; Ferrand, V.; Stoeckli-Evans, H. *J. Chem. Soc., Dalton Trans.* **1997**, 3861–3865.

(13) Adams, R. D.; Kan, Y.; Zhang, Q. *Organometallics* **2011**, *30*, 328−333.
(14) Huq, R.; Poe, A. J.; Chawla, S. *Inorg. Chim. Acta* **1980**, *38*, 121−125.
(15) *SAINT+, version 6.2a*; Bruker Analytical X-ray Systems, Inc., Madison, WI, 2001.
(16) Sheldrick, G. M. *SHELXTL, version 6.1*; Bruker Analytical X-ray Systems, Inc., Madison, WI, 1997.
(17) *ADF2013*; SCM Theoretical Chemistry, Vrije Universiteit, Amsterdam, The Netherlands; http://www.scm.com.
(18) Perdew, J. P.; Ruzsinszky, A.; Csonka, G. I.; Vydrov, O. A.; Scuseria, G. E. *Phys. Rev. Lett.* **2008**, *100*, 136406.
(19) (a) Bau, R.; Drabnis, M. H. *Inorg. Chim. Acta* **1997**, *259*, 27−50. (b) Teller, R. G.; Bau, R. *Struct. Bonding* **1981**, *41*, 1−82.
(20) Adams, R. D.; Captain, B. *Organometallics* **2007**, *26*, 6564−6575.
(21) Haak, S.; Süss-Fink, G.; Neels, A.; Stoeckli-Evans, H. *Polyhedron* **1999**, *18*, 1675−1683.
(22) Mingos, D. M. P. *Acc. Chem. Res.* **1984**, *17*, 311−319.
(23) Adams, R. D.; Captain, B. *Acc. Chem. Res.* **2009**, *42*, 409−418.